

AVERAGE NEUTRON PARAMETERS FROM DIFFERENTIAL ELASTIC SCATTERING  
CROSS SECTIONS OF NEUTRONS WITH ENERGIES BELOW 450 KEV.

Ljudmila V.Mitsyna, Albert B.Popov, George S.Samosvat

Joint Institute for Nuclear Research, Dubna, 141980, USSR

**Abstract:** The paper describes a recently developed method of extracting s- and p-wave neutron strength functions and scattering radii from average differential cross sections measured at the pulsed reactor IBR-30. The results for nuclei in the region  $48 < A < 238$  are compared with other experimental data and theoretical calculations.

(Neutrons, differential cross sections, strength functions, scattering lengths)

Introduction

The possibility of extracting neutron strength functions  $S_j^l$  ( $l$  is the orbital momentum,  $j$  - the total angular momentum of the neutron) and  $R_l^\infty$  parameters for  $l=0,1$  from average differential elastic scattering cross sections of keV-neutrons was first demonstrated in [1]. This method exploits the fact that a cross section averaged over resonances in a given energy range is described within a good accuracy by

$$\langle \sigma(\theta) \rangle = \frac{\sigma_s}{4\pi} [ 1 + \omega_1 P_1(\cos\theta) + \omega_2 P_2(\cos\theta) ],$$
 with coefficients  $\sigma_s(E), \omega_1(E)$  and  $\omega_2(E)$

for even-even target nuclei being easily expressed through the parameters  $S_0^0, S_{1/2}^1, S_{3/2}^1, R_0^\infty$  and  $R_1^\infty$  by averaging one-level resonant expressions. Here  $\omega_2$  accounts also for the contribution from interference between s- and d-wave potential scattering, provided  $R_2^\infty = R_0^\infty$ . In

[2] the above parameterization was generalized to A-odd nuclei, for which in the expressions for  $\sigma_s$  and  $\omega_2$  there appear terms dependent on a common distribution function of partial neutron widths  $\Gamma_{nj}$  for two-channel p-wave resonances. This allowed obtaining of more correct values of parameters for odd nuclei together with some information about correlation between j-channels. In [3] the inclusion in analysis of earlier data on polarizing power of scattering at E=400 keV allowed qualitative observation of spin-orbit splitting of potential scattering phase shift  $\delta_1$ , i.e.

observation of  $R_{11/2}^\infty$  and  $R_{13/2}^\infty$  instead of mean  $R_1^\infty$ .

Method

Measurements by the time-of-flight method were carried out at the IBR-30 reactor in Dubna under a resolution of  $\approx 25$  ns/m. Neutrons scattered from a sample plate 0.002-0.025 barn<sup>-1</sup> thick were detected at angles 45°, 90° and 135° by a battery of <sup>3</sup>He-counters. Data analysis gave  $\langle \sigma(\theta) \rangle$  in the form of  $\sigma_s, \omega_1, \omega_2$  parameters related to  $\approx 20$  energy intervals with mean energy from 1.5 to 442 keV. In addition, densities of neutron widths over 2-8 intervals were calculated from data [4] and expressed as

$$\sum_n \Gamma_n / \Delta E = \sqrt{E} [ S^0 + V ( S_{1/2}^1 + 2S_{3/2}^1 ) ],$$

where  $V = (kR)^2 [ 1 + (kR)^2 ]^{-1}$ ,  $R = 1.35A^{1/3}$  fm and E is in eV. In the analysis of  $\langle \sigma(\theta) \rangle$  for heavy nuclei (starting from Gd) the influence of isotropic inelastic scattering was accounted for with its cross section being parametrized through the sought-for strength functions  $S_j^l$  within the Hauser-Feshbach formalism taking into account the Moldauer fluctuation corrections. The scattering radius in the general case can be defined similar to  $R'_0 = R(1 - R_0^\infty)$  for s-wave:

$$\frac{R'_l}{R} = \frac{\delta_l^0}{\phi_l},$$

where  $\phi_l$  is the phase shift on a hard sphere. Then at  $E \rightarrow 0$  it is

$$R'_l = R [ 1 - \frac{(2l+1)R_l^\infty}{1 + (l + \frac{1}{2})R_l^\infty} ].$$

We work under boundary conditions  $b_l = 1/5$ , which are close to traditional  $b_l = s_l$  ( $s_l$  is the shift factor) or  $b_l = -1$ . They all are the same at  $E \rightarrow 0$  and give  $R'_1 = R(1 - 3R_1^0)$ .

### Results

Up to the present 42 samples have been investigated. The results are partly reported in /5/ and the table lists the remaining ones (including the parameters for  $^{103}\text{Rh}, \text{Ag}, ^{117}\text{Sn}$  and  $^{119}\text{Sn}$  corrected in accordance with /2/).

T a b l e

Tar- get	$S_{1/2}^1$	$S_{3/2}^1$	$R_0^0$	$R_1^0$
Cu	3.0±1.8	1.1±0.6	-0.25±0.06	0.32±0.06
Y	1.2±1.2	5.5±0.5	-0.20±0.03	0.52±0.04
Nb	9.8±1.5	4.4±0.5	-0.23±0.03	0.26±0.03
<sup>92</sup> Mo	2.1±2.4	4.0±0.5	-0.16±0.06	0.21±0.05
<sup>94</sup> Mo	3.2±1.8	4.8±0.4	-0.17±0.04	0.16±0.03
Rh	8.3±1.1	3.1±0.4	0.07±0.03	-0.01±0.03
Ag	5.8±1.0	3.8±0.4	0.02±0.03	-0.05±0.02
In	7.4±0.9	2.5±0.3	0.04±0.02	-0.19±0.01
<sup>117</sup> Sn	4.7±0.9	2.3±0.3	0.11±0.02	-0.22±0.02
<sup>119</sup> Sn	3.8±0.9	1.3±0.2	0.05±0.02	-0.22±0.02
Sb	5.1±1.0	2.2±0.3	0.17±0.03	-0.24±0.03
Nd	3.3±1.4	1.5±0.3	0.13±0.07	-0.11±0.05
Gd	2.6±0.9	2.2±0.3	0.10±0.04	-0.13±0.03
Dy	0.2±0.8	2.2±0.5	-0.09±0.04	-0.11±0.02
Er	2.0±0.9	1.8±0.4	-0.02±0.03	-0.02±0.02
Ta	3.5±0.9	1.7±0.3	0.06±0.03	0.16±0.02
W	3.4±1.0	2.4±0.4	0.09±0.05	0.21±0.03
Re	5.4±1.4	3.0±0.7	0.22±0.05	0.03±0.07
Pt	0.0±0.4	0.7±0.2	-0.20±0.02	0.15±0.02
<sup>238</sup> U	2.0±1.0	1.8±0.5	-0.11±0.03	0.14±0.03

### Comparison

It is interesting to compare the extracted from  $\langle \sigma(\theta) \rangle$  values of  $S^0$ ,  $R'_0$  and  $S^1 = \frac{1}{3} S_{1/2}^1 + \frac{2}{3} S_{3/2}^1$  with the compilation data from /4/. Figures 1 and 2 demonstrate a good agreement of our values for  $S^0$  and  $R'_0$  with those recommended in /4/. Only for nuclei with  $A < 90$  our  $S^0$  values are systematically lower than those in /4/ due to a significant self-shielding effect for strong s-wave resonances.

Since in our case the  $R'_0$  values were determined by using wide energy intervals, they must less experience fluctuations due to resonance statistics, than local  $R'_0$

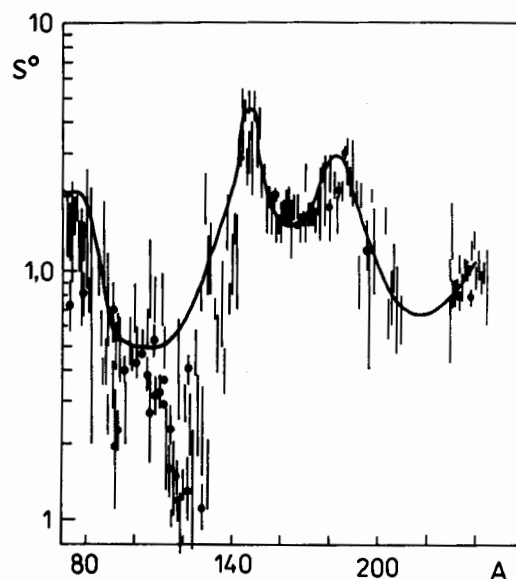


Fig.1.  $S^0$  data. Vertical lines—experimental values from /4/, points—this work data. The curve—calculated behaviour for  $S^0(A)$  also from /4/.

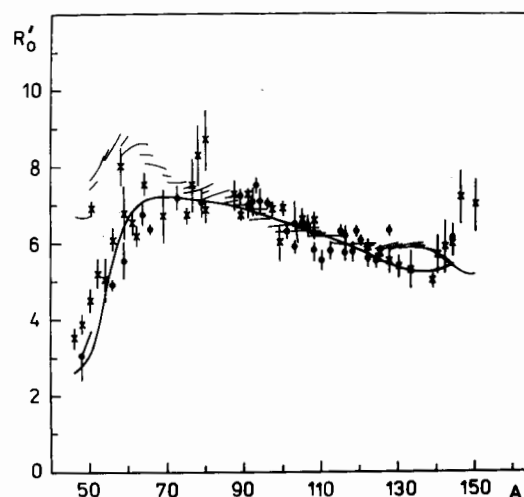


Fig.2.  $R'_0$  in the 3p-resonance region.

Crosses—values from /4/, points—our data, solid curve—OM calculation for Moldauer potential, sections of curves—calculation with the "regional" potential.

values extracted from thermal cross sections or from resonance shapes. Fig.2 shows that both kinds of  $R'_0$  values coincide within error limits and the discrepancy is not bigger than 15%. This fact disagrees with the conclusion of Nikolenko [6] that fluctuations of local  $R'_0$  can reach 100%. Independence of  $R'_0$  of the method of its extraction appears essential for the estimation of recommended values. One may judge agreement of our p-wave strength functions

with literary data by looking at fig.3. It shows that the obtained from  $\langle \sigma(\theta) \rangle$   $S^1$  values agree with a full set of data satisfactorily described by various optical model (OM) calculations.

#### New information

Experimental  $S^1_{1/2}$ ,  $S^1_{3/2}$  and  $R'_1$  values are the new ones. For the first time noncoinciding  $S^1_{1/2}$  and  $S^1_{3/2}$  peaks with the distance between maxima  $\Delta A = 13 \pm 4$  were observed as a function of  $A$ . (This is a first direct observation of spin-orbit splitting of an unbound single particle state.) Besides of that, there is observed a specific behaviour for  $R'_1(A)$  which is an evidence for the extremely weak nonresonant p-wave scattering on nuclei with  $A=60-90$  (see fig.4).

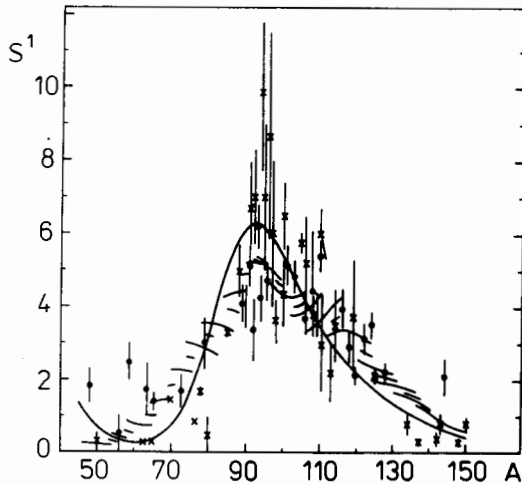


Fig.3.  $S^1$  strength functions. Crosses - from /4/, points - this work, solid curve - OM calculation with the Camarda potential, solid-line sections - for the "regional" potential.

#### OM calculation

The agreement of the above mentioned facts with the OM calculations was checked by using the SCAT-program /7/. We obtained a satisfactory agreement of experimental data with the  $R'_0$ ,  $R'_1$  and  $S^1$  values calculated by using the Moldauer potential /8/ for the s-wave neutron data and its modified by Camarda /9/ version with a larger real term for the p-wave data (with a depth of 1 MeV and a diffuseness of 0.1 fm). Figures 2,3,4 illustrate the results (solid curves). As for the description of the  $S^1_{1/2}$  and  $S^1_{3/2}$  experimental values the

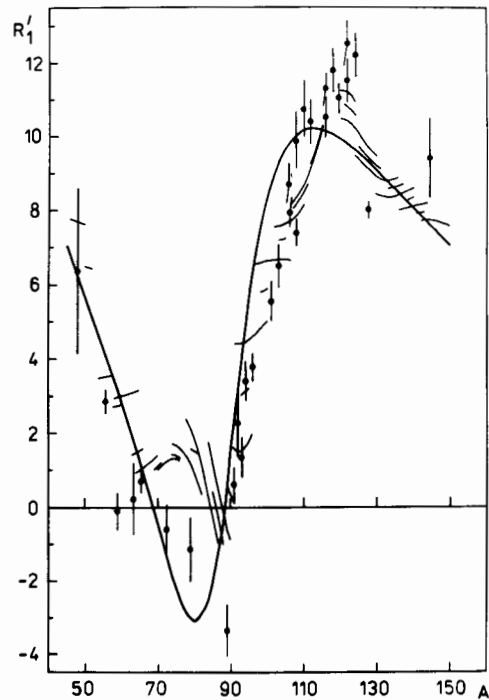


Fig.4. P-wave scattering radii. Solid curve - calculation with the Camarda potential, solid-line sections - with the "regional" potential.

OM calculations with Camarda potential using a conventional spin-orbit term  $V_{so} = 7$  MeV give for the  $S^1_{1/2}$  and  $S^1_{3/2}$  peaks a spacing of  $\Delta A = 6$  only. Calculations were also made with a potential from /10/ named by the authors a "regional" potential (for  $85 < A < 125$ ). This potential is more complicated than the Moldauer-Camarda one since the  $r_0$  parameter ( $R = r_0 A^{1/3}$ ) and parameter of diffuseness entering the Saxon-Woods form factor are taken different for the real and the imaginary part and are the linear functions of  $A$ . Moreover, potential depths contain isospin terms proportional to  $\frac{N-Z}{A}$ , therefore, the calculated  $R'_l$  and  $S^1_j$  are represented in figs. 2, 3, 4, 5 by sections of curves, each corresponding to a given element. Both tested potentials, though providing a satisfactory description for the experimental scattering radii  $R'_0$  and  $R'_1$  and  $S^1$  strength functions, were unable to give explanation for the observed splitting of  $S^1_j$ . The experimental data require  $V_{so} = 10$  MeV. This value is by a

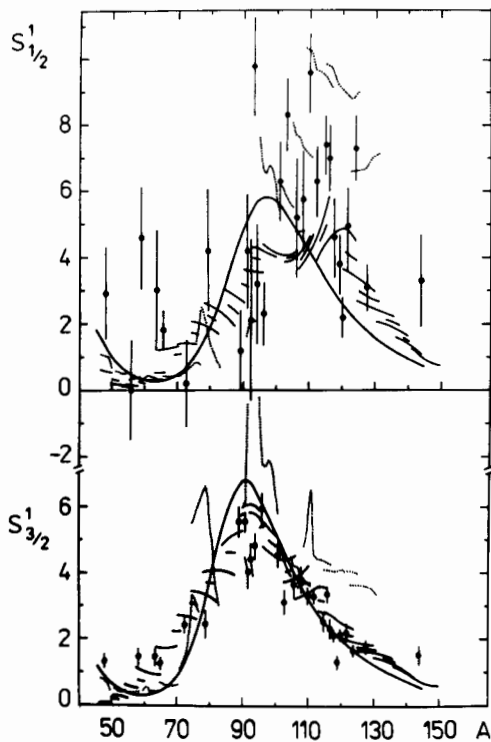


Fig.5.  $S_{1/2}^1$  and  $S_{3/2}^1$  strength functions. Solid curve- Camarda potential, solid-line sections- "regional" potential with  $V=10$  MeV, dotted curve- calculated in /11/.

factor of 1.5-2 larger than that used in most of potentials for the description of bound as well as unbound nuclear states. Just with the fitted value of  $V_{s0}=10$  MeV we have obtained for the "regional" potential the solid-line sections shown in the figures. Calculations have demonstrated also that the conventional spherical OM did not give an explanation for a higher experimental maximum of  $S_{1/2}^1$  with respect to the  $S_{3/2}^1$  peak. Recently the  $S_{1/2}^1$  and  $S_{3/2}^1$  were calculated /11/ in the 3p-single particle resonance region in the frame of the OM which takes into account coupling with many phonon excitations and uses the generally accepted value for the spin-orbit term. The results are presented in fig.5 by dotted curves. Although it is difficult to draw a definite conclusion about agreement of the newly calculated  $S_j^1$  values with experimental data, they look like being in better correspondence with the observed splitting of the  $S_{1/2}^1$  and  $S_{3/2}^1$  peaks and

correlation of their maxima. In this model variations in phonon coupling strength from nucleus to nucleus result in a different from the conventional OM behaviour for the  $S_j^1(A)$ . An idea to calculate  $R_1'$  within this approach looks attractive.

#### References

1. V.G. Nikolenko et al: Proceed. Int. Conf., Antwerp, 6-10 Sept, 1982, p. 781
2. A.B. Popov, G.S. Samosvat: *Jadern. Fiz.*, **45**, 1522 (1987)
3. A.B. Popov, G.S. Samosvat: *JINR Rap. Comm. N° 18-86*, 30, Dubna (1986)
4. S.F. Mughabghab et al: Neutron cross sections, A.P., v.1, part A (1981); part B (1984)
5. A.B. Popov, G.S. Samosvat: Proceed. Int. Conf. Santa Fe, 13-17 May, 1985, v.1, p. 621
6. V.G. Nikolenko: *JINR*, P4-81-351, Dubna (1981)
7. A.B. Smith: *Comp. Phys. Comm.*, **1**, 135 (1969)
8. P.A. Moldauer: *Nucl. Phys.*, **47**, 65 (1963)
9. H.S. Camarda: *Phys. Rev.*, **C9**, 28 (1974)
10. A.B. Smith et al: *Nucl. Phys.*, **A415**, 1 (1984)
11. V.V. Samojlov, M.G. Urin: *Izvestija AN USSR, Ser. Fiz.*, **52**, 161 (1988)